

# Conventional Multiple Degree-of-Freedom Array Models

*M. Folley<sup>\*</sup>, D. Forehand<sup>†</sup>*

<sup>\*</sup>School of Planning, Architecture and Civil Engineering, Queen's University Belfast, Belfast, Northern Ireland

<sup>†</sup>School of Engineering, University of Edinburgh, Edinburgh, United Kingdom

## 8.1 INTRODUCTION AND FUNDAMENTAL PRINCIPLES

This chapter considers the modelling of wave energy converter (WEC) arrays as an extension of the modelling of isolated WECs. From a fundamental numerical modelling perspective, the modelling of a WEC array can be considered identical to the modelling of a single WEC with multiple degrees-of-freedom. This can be seen clearly by recognizing that an array could be considered as a single entity with multiple modes (WECs) from which energy is extracted. For example, the Manchester Bobber, which consists of multiple heaving buoys all mounted on a single platform, could equally be considered as a single WEC with multiple buoys or as a WEC array of individual buoys. Thus, all of the modelling tools described in Parts A and B of this book, which are available for modelling isolated WECs, are also available for WEC arrays. Furthermore, all of the assumptions, capabilities and limitations that apply to the particular modelling tools when used to simulate single WECs are also relevant when those methods are applied to modelling WEC arrays.

Although the vast majority of initial WEC array models were based on semianalytical models (see [Chapter 9](#)), as computational resources have increased there has been an increase in the production of WEC array models that are effectively extensions of methods applied to single WECs. An early example of the extension of a single WEC modelling technique to an array was published by [Falcao \(2002\)](#). In this case an analytical frequency-domain model of an oscillating water column (OWC) was extended to an infinite array of OWCs. It was shown that with phase control (see [Chapter 12](#)) the array can change the capture factor significantly compared to an isolated OWC, but without phase control the change in capture factor due to the array was typically minimal.

By 2008 computational resources had increased so that analytical solutions were not needed and numerical models based on a boundary element method (BEM) became possible. [Taghipour and Moan \(2008\)](#) used generalized modes in WAMIT ([WAMIT, 2011](#)) to model a 21-buoy array, whilst a 25-buoy version of the Manchester Bobber was modelled by [Thomas et al. \(2008\)](#). In both of these cases a frequency-

domain model was used, with the latter also including a comparison to experimental results. It was found that the modelled response of the WEC array was ‘qualitatively’ similar to the measured response, but divergence occurred close to the natural frequencies of the buoys. Another frequency-domain WEC array model using hydrodynamic coefficients generated from a BEM was reported by [Vicente et al. \(2009\)](#), where an array of 3 buoy-type WECs with a complex mooring arrangement was modelled.

Frequency-domain WEC array models have also been used for optimization studies. [Bellew et al. \(2009\)](#) used a frequency-domain WEC array model to optimize the damping coefficients for a rectilinear array of 5 heaving buoys. [Cruz et al. \(2009\)](#) used a similar model to investigate the optimum array layout for a 4-buoy array in irregular spread waves. The model indicated that an increase in the average capture factor of 4% was possible compared to a single WEC. Although this is much less than may be suggested from models using regular waves, it is not an insignificant change in power capture. A similar result was also found by [Folley and Whittaker \(2009\)](#) who used a frequency-domain model to investigate the maximum increase in power capture for an array and its sensitivity to control parameters. However, Folley and Whittaker also found that the performance of an array is typically very sensitive to control parameters, so that only a small deviation from an optimal control strategy can result in a significant loss of power capture. A final example of a frequency-domain WEC array model is reported by [Borgarino et al. \(2012\)](#), who looked at the magnitude of array interactions at large separation distances. Borgarino et al. found that even at large separations of over 1000 m the interaction factor could still be significant.

Reported examples of time-domain WEC array models are significantly less common than those for frequency-domain WEC array models. This reflects the increased complexity in time-domain models, both requiring additional analytical and computational resources, compared to frequency-domain models. Moreover, this

additional complexity is even greater for time-domain WEC array models compared to frequency-domain WEC array models, as will be shown in [Section 8.2.2](#). [Babarit et al. \(2009\)](#) reports a time-domain WEC array model for two heaving buoys. A time-domain model was used by Babarit et al. because the modelled power take-off (PTO) consisted of a hydraulic cylinder, which has a non-linear characteristic. Because the systems are different it is not possible to compare the results from this time-domain WEC array model with those of the frequency-domain WEC array models quantitatively; however, the general characteristics appear to have been replicated. Another hydrodynamic time-domain WEC array model is reported in detail in [Forehand et al. \(2016\)](#). In that paper, an array of four heaving buoys with hydraulic PTOs and connected to an electrical network is modelled. Simulations are performed to investigate the effect of buoy interactions and the control strategy on the electrical network and to explore the influence of network faults on the buoy responses. The same hydrodynamic array model was also used by [Nambiar et al. \(2015\)](#) to predict the optimal resistive and reactive control parameters for a three-float Wavestar device ([Hansen and Kramer, 2011](#)) with PTO force constraints and in a range of irregular sea-states.

Only a single example of the use of a spectral-domain WEC array model has been published. In this paper [Folley and Whittaker \(2013\)](#) model an array of 24 heaving buoys that are each damped by a Coulomb friction brake. The results of the spectral-domain WEC array model are compared to those obtained from wave-tank experiments for three different array configurations. It was found that the average array power capture predicted by the model was similar to that measured in the wave-tank experiments, but that there could be relatively large differences between the predicted and measured power capture for individual buoys, which may be attributable to wave-tank aberrations ([Lamont-Kane et al., 2013](#)).

Finally, a computational fluid dynamics (CFD) model of an array of two heaving buoys

is reported by [Agamloh et al. \(2008\)](#). In this paper a commercial CFD code is used to model a numerical wave tank that contains the two heaving buoys. The results of the CFD model show that there is interaction between the buoys; however, there is no discussion of the validity of the results and the authors recognize that further simulations are required to fully understand the results obtained.

It can be seen from the preceding short review of the literature that the same techniques used to model single WECs have been used regularly to model WEC arrays. It will be noted that these papers were typically written with an objective distinct from the verification or validation of the WEC array model. Consequently, there is little discussion in the papers regarding how best to construct the WEC array model and how to interpret the results. However, although the extension of the modelling tools from single WECs to WEC arrays is conceptually simple, additional issues exist for the modelling of WEC arrays over and above those for the modelling of single WECs. Issues associated with the modelling of WEC arrays using the same modelling techniques as for single WECs can be conveniently separated into those associated with models based on linear potential flow and those associated with other models: specifically Parts A and B of this book, respectively. In many cases the issues that arise can be resolved, or at least made acceptable, provided that the model is designed appropriately. However, some issues are more fundamental and effectively limit the use of the particular modelling technique in its application to WEC arrays. These methods of resolution and the fundamental limitations of particular techniques are discussed in the following sections.

## 8.2 MODELLING BASED ON LINEAR POTENTIAL FLOW

It can be seen from the review of the literature that the vast majority of WEC array models based on extensions of single WEC models are

themselves based on linear potential flow theory. The principal issue for the modelling of WEC arrays using a model based on linear potential flow theory is the computational processing requirements. Compared to single WECs, the computational processing requirements for a WEC array increase due to:

- a greater complexity of the linear potential flow solution at each wave frequency,
- a greater number of wave frequency components that are required to represent the hydrodynamic coefficients accurately,
- a greater complexity of the equations of motions that need to be solved.

Let us first consider the computational effort required for the linear potential flow solution. Except for a few idealized shapes, which are unlikely to be sufficiently accurate to be used in a model of a WEC, a BEM is required to generate the hydrodynamic coefficients necessary for a frequency-domain, time-domain or spectral-domain model. A good rule-of-thumb is that for each frequency the required computational effort for a BEM increases with the number of panels squared. Thus, for example, generating the hydrodynamic coefficients for a 10 WEC array would take approximately 100 times longer than for a single WEC of the same type for each wave frequency computed. This means that when generating the hydrodynamic coefficients for WEC arrays, it is typically beneficial to analyse, by solution convergence or otherwise, the relationship between the number of panels used to model each WEC and the accuracy of the linear potential flow solution.

Next consider the number of frequencies for which hydrodynamic coefficients need to be computed in order to produce an accurate model of a WEC array. The maximum and minimum frequencies can be defined by the range of frequencies at which the response is significant; however, the minimum acceptable frequency resolution requires slightly more consideration. Avoiding the definition of a complicated condition for an acceptable discretization, it is

reasonable to assert that the resolution should be sufficient so that the frequency dependence of the hydrodynamic coefficients can be well replicated either using a linear interpolation or more coarsely as a step-wise variation.

The typical frequency dependence of a single WEC's hydrodynamic coefficients means that 20–30 frequency components are normally sufficient. However, the frequency dependence for the hydrodynamic coefficients in a WEC array is generally more complex. Fig. 8.1 shows the frequency dependence of the radiation damping coefficients for an array of two 20 m diameter pitching cylinders separated by 150 m. It can be seen that whilst the auto-coupling radiation coefficient associated with the force on each buoy that is due to its motion and in-phase with

its own velocity is relatively well behaved, the cross-coupling radiation coefficient associated with the force on one buoy due to the motion of the other buoy and in-phase with its velocity is much more complex. In particular, it can be seen that the value of this cross-coupling radiation coefficient oscillates, with the frequency of this oscillation increasing with wave frequency.

The reason for this characteristic oscillation of the cross-coupling radiation damping coefficient can be understood by considering the fundamental hydrodynamics of the coupling and the definition of the cross-coupling radiation coefficient, which is the ratio of the force on one buoy in-phase with the velocity of the other buoy. However, the force is not directly due to the other buoy's velocity, but due to the wave

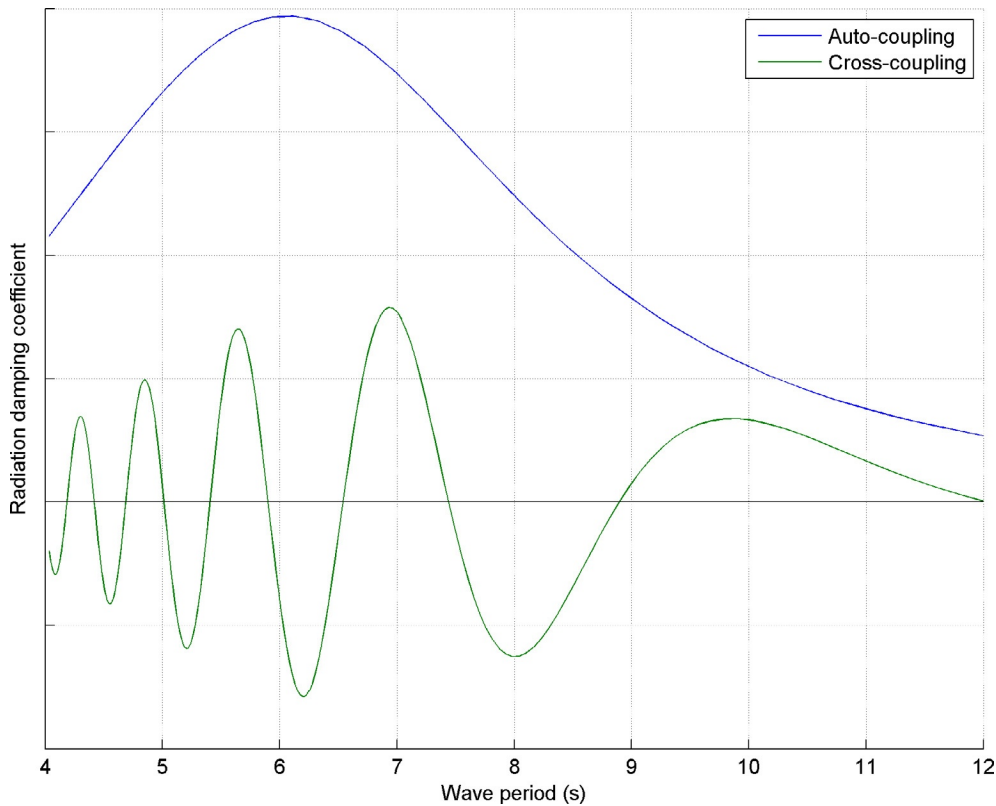


FIG. 8.1 Radiation coefficients for two WEC array.

generated by the other buoy's movement. Thus, if the force due to the radiated wave and velocity are in-phase it is a finite positive radiation coefficient, but if they are 90 degrees out-of-phase the radiation coefficient becomes zero (similarly, if they are 180 degrees out-of-phase the radiation coefficient is negative and at 270 degrees it becomes zero again). Thus, the cross-coupling radiation coefficient oscillates approximately with the phase of the radiated wave at the location of the second buoy, which changes more rapidly as the wave frequency increases, as observed in Fig. 8.1.

Fig. 8.2 shows an estimate of the number of frequency components required for a deep-water WEC array model as it varies with maximum WEC separation and maximum wave frequency (the minimum wave frequency has

a relatively small influence on the number of frequency components required). In this figure it is assumed that the cross-coupling coefficient can be reasonably approximated with ten discrete frequencies for each oscillation of the coefficient. For example, if the maximum WEC separation is 500 m and the maximum wave frequency is 0.25 Hz (a wave period of 4.0 s) then a total of approximately 200 frequency components is required to model the WEC array accurately.

This increase in the number of frequency components, in combination with the increase in the computational effort for each wave frequency, means that generating the hydrodynamic coefficients for a WEC array is significantly more demanding than for a single WEC. Indeed, the computational requirements may become so large, particularly for geometrically

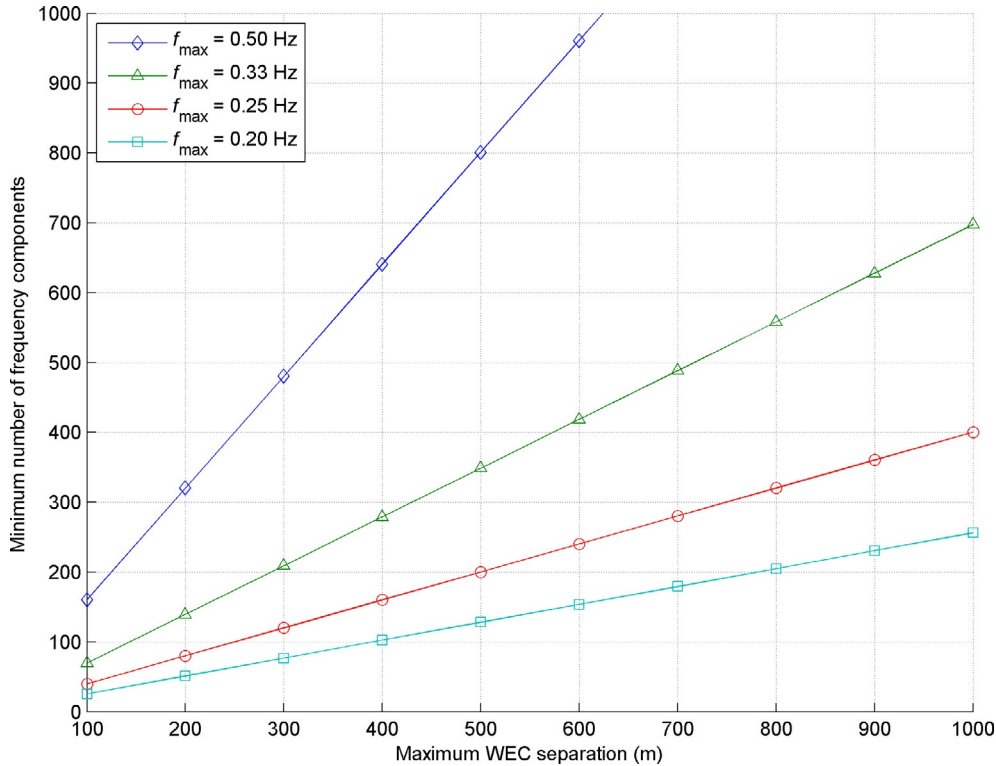


FIG. 8.2 Minimum number of frequency components for WEC array model.

dispersed WEC arrays, that a further approximation may be necessary; specifically, a reduction in the number of frequency components (as the computational effort in the BEM is difficult to reduce significantly). It can be argued that, provided the oscillations of the hydrodynamic coefficients are uncorrelated to the reduced set of frequency components, then the estimated output of the WEC array model should be unbiased, albeit with an increase in uncertainty. Calculating this uncertainty is beyond the scope of this book (although an estimate can be made from a convergence test), but will sensibly increase with the reduction in the number of frequency components.

Following the generation of the hydrodynamic coefficients using a BEM, these parameters are used in the equations of motion to calculate the WEC array response. However, whilst they can be used directly in both frequency-domain and spectral-domain models, their use in a time-domain model requires further processing. Consequently, these two types of models are discussed separately in the following subsections.

### 8.2.1 Frequency-Domain and Spectral-Domain Modelling

Frequency-domain and spectral-domain models use the frequency-dependent hydrodynamic coefficients directly in their equations of motion, as described in detail in [Chapters 2 and 4](#), respectively. The key difference between a WEC array model and a single WEC model is the number of degrees-of-freedom (or modes) for which the system needs to be solved. In this respect, it is worth noting that for single WECs it is possible, in particular circumstances, to ignore some degrees-of-freedom because they do not influence the output. For example, surge can often be ignored when only the response of a single WEC in heave is required. This is because there is no hydrodynamic coupling between heave and surge and thus it would only be

necessary to model surge if there were some structural coupling due to, for example, the mooring configuration. This lack of hydrodynamic coupling between heave and surge is often used to minimize the effort in modelling a single WEC. However, this cannot be applied to a WEC array as the surge on one WEC will couple with the heave of another WEC due to the radiated waves. Consequently, the degrees-of-freedom of a WEC array model will be at least the number of WECs times the degrees-of-freedom of the same single WEC model, and possibly significantly more. Notwithstanding the inevitable and significant increase in degrees-of-freedom for a WEC array, the WEC array models are typically easily solved because the dominant dynamic force on each WEC in the array is due to its own motion. Thus, the equations of motion tend to be diagonally dominant, which can generally be solved efficiently.

### 8.2.2 Time-Domain Modelling

In a time-domain model the frequency-dependent hydrodynamic coefficients are not used directly in a WEC array model, but instead used to generate either convolution integrals (as in Cummins equation) or a higher-order model. The processes of generating the convolution integrals or the higher-order model are described in detail in [Chapter 3](#). Here we focus on the additional issues that may arise in their use in the modelling of WEC arrays and to do so each of the different types of time-domain model is considered separately.

In the time-domain models based on the Cummins equation, the frequency-dependent hydrodynamic coefficients are used to produce the impulse response functions that form part of the kernels of the convolution integrals. It is worth reiterating that an impulse response function is required for each cross-coupling component and so the number of these is equal to the number of degrees-of-freedom squared.



However, only about half of these are unique due to the symmetric nature of the interactions (the radiation impulse response function between modes  $i$  and  $j$  is the same as the radiation impulse response function between modes  $j$  and  $i$ ). As previously described (see [Chapter 3](#)), the impulse response functions are generated in preprocessing at each time-step by integrating, with respect to frequency, the product of the radiation damping coefficient and the cosine of the product of frequency and time. Thus, the accuracy of the impulse response functions depends on the frequency resolution relative to the frequency-dependent variations in the hydrodynamic coefficients. However, as noted earlier, a high frequency resolution, resulting in a large number of frequency components, is typically required to capture all the variations in the hydrodynamics coefficients and a lower frequency resolution, which may be used due to limited computational resources, will result in errors in the impulse response functions.

A further point to consider in generating the cross-coupling impulse response functions is that their duration will typically be longer than those for a single WEC. This is because the cross-coupling impulse response functions effectively include the time for the waves to propagate between the WECs in the array. This increased impulse response function duration will result in an increase in the computational effort for solving the WEC array model because the lengths of the convolution integrals, which must be calculated each time-step, are equal to the lengths of the impulse response functions.

The alternative to modelling the WEC array using the Cummins equations is to effectively replace the convolution integrals with higher-order models, where additional degrees-of-freedom have been added that result in an equivalent response to the convolution integrals. The same methods as for a single WEC (described in [Chapter 3](#)) can be used to produce the higher-order models; however, the increase in number of higher-order models required

and their increased complexity associated with the greater variability of the hydrodynamic coefficients, means that more consideration is required with respect to the stability of these higher-order models. Whilst for a single WEC it may be possible to identify a stable higher-order model using trial-and-error, this is not feasible when a WEC array may contain hundreds of higher-order models.

A method designed to produce more stable higher-order models of WEC arrays is detailed by [Forehand et al. \(2016\)](#). In that approach, the radiation impulse response functions do not need to be calculated. Instead, each frequency-dependent radiation impedance function  $K_{ij}(\omega)$  is first approximated by a *rational* transfer function, as in [McCabe et al. \(2005\)](#). The function  $K_{ij}(\omega)$  is defined to be:

$$K_{ij}(\omega) = B_{ij}(\omega) + i\omega(A_{ij}(\omega) - A_{ij}(\infty)),$$

where  $A_{ij}(\omega)$  and  $B_{ij}(\omega)$  are the added mass and added damping coefficients. The orders  $n$  and  $m$  of the numerator and denominator polynomials, respectively, of the approximating transfer function are then systematically increased, with  $n < m$ , until the relative root-mean-square error between the transfer function and  $K_{ij}(\omega)$  is less than a prescribed value (e.g.  $<1\%$ ).

As an example, [Fig. 8.3](#) shows an array of six *heaving* buoys arranged in a rectangular pattern and in 20 m water depth. The buoys are hemispheres with radius  $r=3$  m and with a centre-to-centre spacing of 9 m in both the  $x$  and  $y$  directions.

[Fig. 8.4](#) shows the real part of both  $K_{ij}(\omega)$  and its approximating transfer function  $H(\omega)$  for the radiation interaction between buoy 1 and buoy 3. Note, because of the sequential ordering of the degrees-of-freedom within an array of rigid body WECs, mode 3 is heave of buoy 1, mode 9 is heave of buoy 2, mode 15 is heave of buoy 3, etc. [Fig. 8.5](#) shows the corresponding imaginary part of both  $K_{ij}(\omega)$  and its approximating transfer function  $H(\omega)$  for the radiation interaction between buoys 1 and 3.

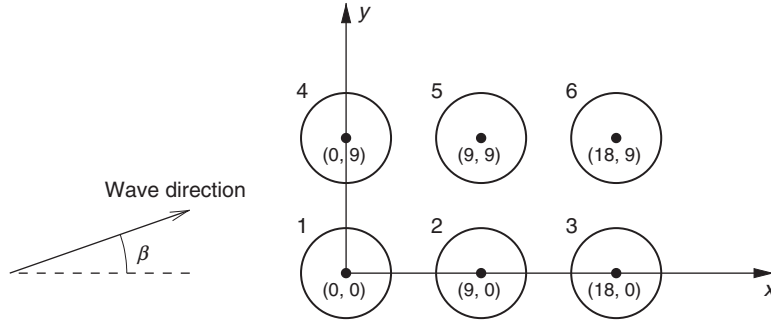


FIG. 8.3 Array configuration for six heaving buoy.

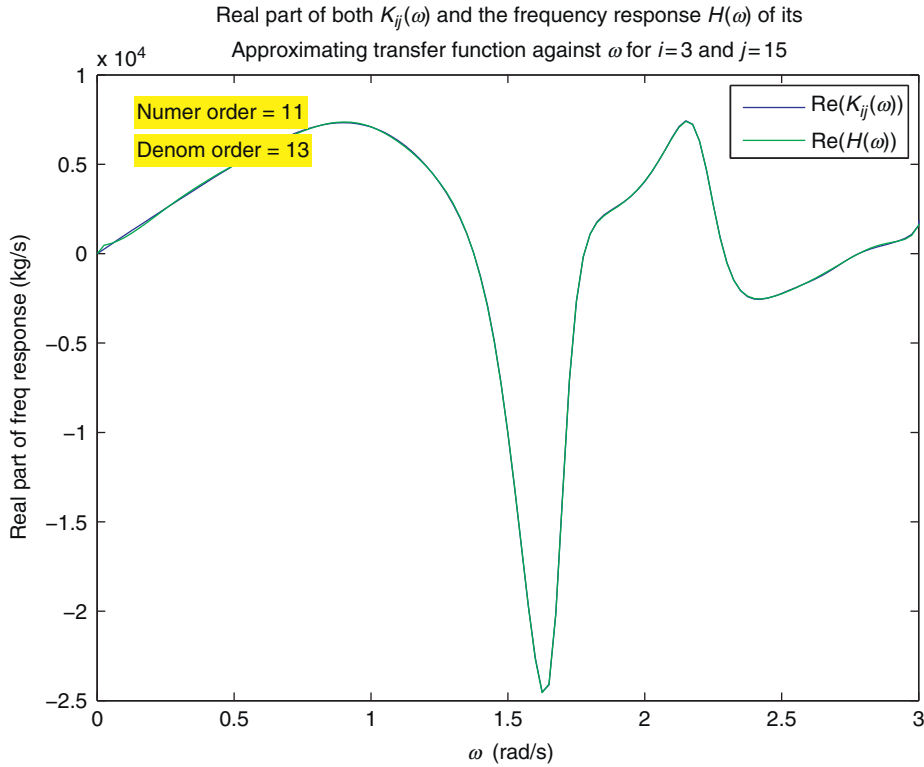


FIG. 8.4 Comparison of real part of transfer function for the radiation interaction between buoy 1 and buoy 3.

Once all the, possibly, high-order, approximating transfer functions have been obtained, the next step is to convert this *whole* system of functions to a *single* equivalent, probably very high-order, state-space model.

As mentioned previously, these extremely large-scale state-space models can be numerically unstable and this is due to number overflow and truncation errors resulting from the finite precision of computer arithmetic.



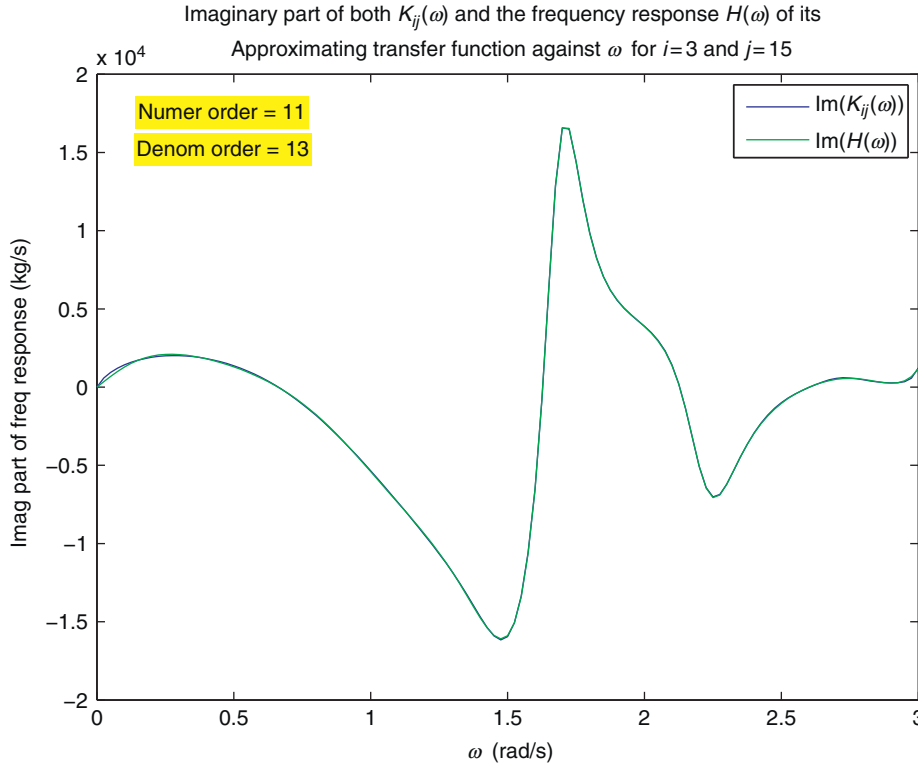


FIG. 8.5 Comparison of imaginary part of transfer function for the radiation interaction between buoy 1 and buoy 3.

The solution proposed by Forehand et al. (2016) is to first convert the approximating transfer functions to zero-pole-gain form by factorizing their numerator and denominator polynomials. The resulting system of zero-pole-gain models is then converted to a state-space model in what is called *modal* canonical form, which is typically far more numerically stable.

In order to verify that the derived hydrodynamic time-domain array model is performing as it should, the steady-state amplitude of the buoy responses to a sinusoidal incident wave can be compared to the corresponding response amplitude operators (RAOs) from the frequency-domain model, over all incident wave frequencies  $\omega$  and wave directions  $\beta$ . The reason for considering multiple incident wave directions is in order to allow the simulation of

irregular spread seas and even if a WEC is axisymmetric, its response in a general array to different wave directions will not be.

For the example problem, Fig. 8.6 refers to the heave of buoy 5 (ie, mode 27) and shows three surface plots. The top plot shows the magnitude (amplitude) of the WAMIT (frequency-domain) RAOs for all incident wave frequencies and directions. The middle plot shows the relative error in amplitude between the time-domain and WAMIT RAOs for all incident wave frequencies and directions. The bottom plot shows the error in phase (in degrees) between the time-domain and WAMIT RAOs for all incident wave frequencies and directions.

The nonsymmetric response of this buoy, with respect to wave direction, can be seen in the top plot in Fig. 8.6. The largest errors

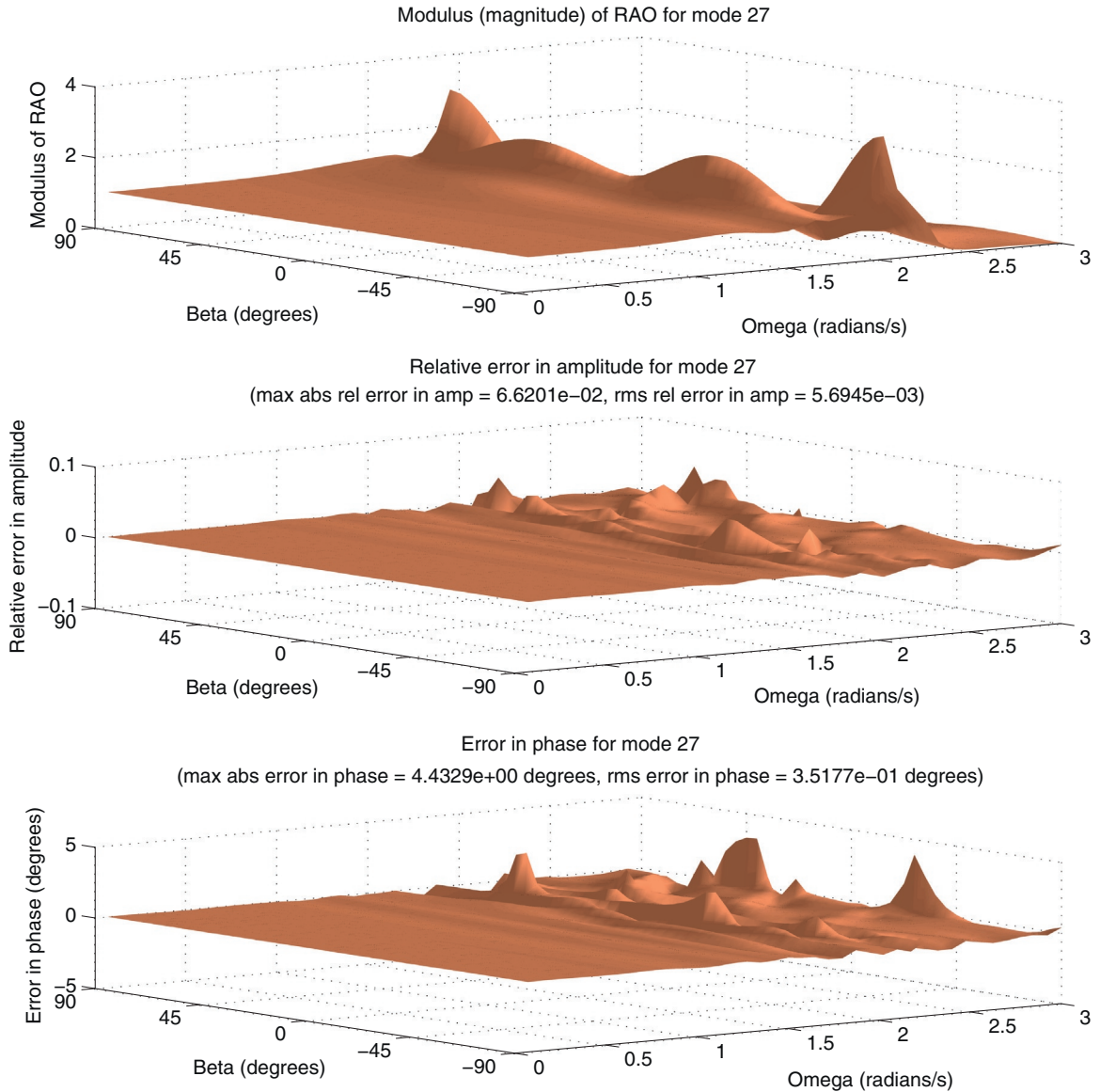


FIG. 8.6 Response amplitude operator (RAO) for buoy 5 together with the error in amplitude and phase in the time-domain model.

in amplitude and phase occur around the resonant frequency of the buoys (approximately 1.8 rad/s) and also occur for the highest frequencies, where the response of the buoys is small. The errors at the highest frequencies are

also caused by the fact that steady-state conditions take a long time to be reached for these frequencies and are not quite obtained by the end of the time-domain simulations. A total of 40 wave frequencies and 41 wave directions were

used to produce Fig. 8.6 and this corresponds to  $40 \times 41 = 1640$  time-domain simulations.

Notwithstanding the preceding method to improve the stability of a state-space model, in general the greater the order of the higher-order model the more likely it is to be unstable due to the increase in the number of eigenvalues of the state, or system, matrix (ie, roots of the system's characteristic equation), any of which could be unstable. However, there is still the requirement that the higher-order model adequately represents the frequency-dependent hydrodynamic coefficients in the time-domain. The greater variability of these hydrodynamic coefficients means that typically the order of the higher-order model will need to be greater for a WEC array than for a single WEC. Thus, there is typically a requirement to balance the stability of the higher-order model with the accuracy of its representation.

A higher-order method that has been used in modelling single WECs and deserves additional comment is Prony's method (Clément and Babarit, 2012). Prony's method replaces the impulse response function by the sum of complex exponential functions, with the convolution integral subsequently replaced by additional states. However, the sum of complex exponential functions can only easily represent a decaying function where its initial value is also its maximum value. Whilst this is a reasonable representation for the impulse response function of a single WEC, it is not able to adequately represent the cross-coupling impulse response functions, where the initial value is close to zero and the maximum value occurs a finite period after the start. Thus, Prony's method does not appear to be suitable for modelling WEC arrays.

Another interesting approach, which relates especially to the high-frequency oscillations in the cross-coupling hydrodynamic parameters for widely spaced arrays seen in Section 8.2 (and Fig. 8.1), is presented in the paper by Isberg et al. (2015). In that study a solution is obtained for the motion of an array of WECs

subject to linear PTO forces. Since this problem is purely linear, a frequency-domain approach could have been used but instead the time-domain equations of motion are solved. This solution process does not use the Cummins equation or the higher-order models mentioned previously, but instead is based on the frequency-dependent transfer functions which link the motion of each device to the free-surface elevation at the origin. The interesting aspect of this approach is the way it deals with the problem caused by the high-frequency oscillation in these transfer functions for devices located far from the origin by analytically removing these oscillations.

The final method discussed in this subsection is that reported in Bacelli and Ringwood (2015). In that paper the authors present a method which can be used to investigate the optimal control of WECs and WEC arrays subject to position and force constraints. The method works by first expanding both the WEC motions and PTO forces in a set of suitable basis functions and then the hydrodynamic time-domain equations of motion are solved using a Galerkin approach (Finlayson and Scriven, 1966).

### 8.3 MODELLING BASED ON OTHER TECHNIQUES

Only a single example of WEC array models based on the extension of single WEC modelling techniques other than linear potential flow models is known to be published (Agamloh et al., 2008). However, this lack of examples of WEC array models based on nonlinear potential flow or CFD models is likely to be more related to the limited use of these types of models for modelling WECs in general rather than a specific issue with WEC array models based on these techniques. In particular, the use of nonlinear potential flow models and CFD models has been proposed for WEC array modelling (Folley et al., 2012).

In common with WEC array models based on linear potential flow theory, the principle issue with WEC array models based on nonlinear potential flow or CFD models is the increase in the computational requirements. This could be considered as a particularly challenging issue because these models already require significant computational resources to model a single WEC (see [Chapter 6](#)). However, unlike the BEM used in linear potential flow models, where the effort largely increases with the square of the number of WECs, the computational effort of WEC array models based on nonlinear potential flow or CFD models is approximately linearly proportional to the area or volume of the sea that is being modelled. Thus, a closely packed WEC array will require a smaller increase in computational effort than a spatially dispersed WEC array.

A further and potentially more fundamental issue for WEC array models based on CFD is internal numerical dissipation when resolving the propagation of gravity waves ([Maguire, 2011](#)). The effect of internal numerical dissipation is that the incident wave amplitude tends to decrease as it propagates and so is not constant across the whole modelling domain. This may not be a significant issue when modelling a single WEC since the model could be calibrated so that the incident wave has the desired profile at the location of the WEC; however, for a WEC array this is not possible. A consequence is that the incident wave amplitude could be different for each WEC in the array, which would make it difficult to identify any WEC array interactions as they need to be distinguished from any changes due to the differing incident wave. Moreover, the waves radiated by the WECs will be similarly affected, with more subtle but equally problematic consequences. However, more recently a number of CFD models have been developed that are less prone to internal numerical dissipation ([Qian et al., 2006](#); [Spinneken et al., 2012](#)), which may

reduce the significance of this issue for CFD-based WEC array models.

## 8.4 LIMITATIONS

From the discussions in the previous section it is clear that a general limitation for all array models based on an extension of the modelling used for single WECs is the increase in computational requirements. This is in addition to the limitations inherent in the particular single WEC modelling techniques that are being used as detailed in the appropriate chapter of Parts A and B. For small arrays this increase in computational requirements may be tolerable; however, it is clear that as the array size increases the use of the same modelling techniques as used for single WECs becomes less viable. Additional limitations are associated with the extension of the particular modelling technique being used.

In WEC array time-domain models based on linear potential flow theory the Prony's representation of the impulse response function cannot be used because it is not capable of adequately representing the cross-coupling hydrodynamic forces. In addition, there is a greater tendency for higher-order representations of the hydrodynamics in WEC arrays to become unstable, which requires special consideration and results in an associated limitation on how a higher-order model can be constructed and formulated.

The suitability of WEC array CFD models depends on the amount of internal dissipation with the propagation of gravity waves; some CFD models have been found to have an unacceptable amount of internal numerical dissipation. Consequently, acceptable WEC array CFD models are limited to those based on a CFD scheme that has been shown to have a sufficiently small rate of internal numerical dissipation so that any difference in power capture in the WEC array can be clearly distinguishable from differences due to internal numerical dissipation.

## 8.5 SUMMARY

- Models based on simple extensions to the modelling of single WECs have been used extensively for modelling WEC arrays.
- The computational requirements are significant for large arrays so these techniques are typically limited to small arrays (up to about 10 devices).
- The number of frequency components required to accurately represent a WEC array's hydrodynamics increases significantly relative to a single WEC and depends on the maximum nondimensional separation of the WECs in the array.
- All degrees-of-freedom, including nongenerating modes, should be included in a WEC array model
- Internal numerical dissipation can be an issue for some CFD-based WEC array models.

## References

- Agamloh, E.B., Wallace, A.K., et al., 2008. Application of fluid-structure interaction simulation of an ocean wave energy extraction device. *Renew. Energy* 33 (4), 748–757.
- Babarit, A., Borgarino, B., et al., 2009. Assessment of the influence of the distance between two wave energy converters on the energy production. In: 8th European Wave and Tidal Energy Conference, Uppsala, Sweden.
- Bacelli, G., Ringwood, J.V., 2015. Numerical optimal control of wave energy converters. *IEEE Trans. Sustain. Energy* 6 (2), 294–302.
- Bellew, S., Stallard, T., et al., 2009. Optimisation of a heterogeneous array of heaving bodies. In: 8th European Wave and Tidal Energy Conference, Uppsala, Sweden.
- Borgarino, B., Babarit, A., et al., 2012. Impact of wave interactions effects on energy absorption in large arrays of wave energy converters. *Ocean Eng.* 41, 79–88.
- Clément, A.H., Babarit, A., et al., 2005. The SEAREV wave energy converter. In: 6th European Wave and Tidal Energy Conference, Glasgow, UK, pp. 81–90.
- Clément, A.H., Babarit, A., 2012. Discrete control of resonant wave energy devices. *Phil. Trans. R. Soc. A* 370 (1959), 288–314.
- Cruz, J., Sykes, R., et al., 2009. Wave farm design: preliminary studies on the influences of wave climate, array layout and farm control. In: 8th European Wave and Tidal Energy Conference, Uppsala, Sweden.
- Falcao, A.F.D.O., 2002. Wave-power absorption by a periodic linear array of oscillating water columns. *Ocean Eng.* 29, 1163–1186.
- Finlayson, B.A., Scriven, L.E., 1966. The method of weighted residuals—a review. *Appl. Mech. Rev.* 19, 735–748.
- Folley, M., Whittaker, T.J.T., 2009. The effect of sub-optimal control and the spectral wave climate on the performance of wave energy converter arrays. *Appl. Ocean Res.* 31 (4), 260–266.
- Folley, M., Babarit, A., et al., 2012. A review of numerical modelling of wave energy converter arrays. In: 31st International Conference on Ocean, Offshore and Arctic Engineering, Rio de Janeiro, Brazil.
- Folley, M., Whittaker, T., 2013. Preliminary cross-validation of wave energy converter array interactions. In: 32nd International Conference on Ocean, Offshore and Arctic Engineering, Nantes, France.
- Forehand, D.I.M., Kiprakis, A.E., et al., 2016. A fully-coupled wave-to-wire model of an array of wave energy converters. *IEEE Trans. Sustain. Energy* 7 (1), 118–128.
- Hansen, R.H., Kramer, M.M., 2011. Modelling and control of the Wavestar prototype. In: 9th European Wave and Tidal Energy Conference, Southampton, UK.
- Isberg, J., Engström, J., et al., 2015. Control of rapid phase oscillations in the modelling of large wave energy arrays. *Int. J. Mar. Energy* 11, 1–8.
- Lamont-Kane, P., Folley, M., et al., 2013. Investigating uncertainties in physical testing of wave energy converter arrays. In: 10th European Wave and Tidal Energy Conference, Aalborg, Denmark.
- Maguire, A.E., 2011. Geometric design considerations and control methodologies for absorbing wavemakers. Ph. D. Thesis, The University of Edinburgh.
- McCabe, A.P., Bradshaw, A., et al., 2005. A time-domain model of a floating body using transforms. In: 6th European Wave and Tidal Energy Conference, Glasgow, UK.
- Nambiar, A.J., Forehand, D.I.M., et al., 2015. Effects of hydrodynamic interactions and control within a point absorber array on electrical output. *Int. J. Mar. Energy* 9, 20–40.
- Qian, L., Causon, D.M., et al., 2006. A free-surface capturing method for two fluid flows with moving bodies. *Proc. R. Soc. A* 462 (2065), 21–42.
- Spinneken, J., Heller, V., et al., 2012. Assessment of an advanced finite element tool for the simulation of fully-nonlinear gravity water waves. In: 22nd International Ocean and Polar Engineering Conference, Rhodes, Greece.
- Taghipour, R., Moan, T., 2008. Efficient frequency-domain analysis of dynamic response for the multi-buoy wave

- energy converter in multi-directional waves. In: 18th International Offshore and Polar Engineering Conference, Vancouver, Canada.
- Thomas, S., Weller, S., et al., 2008. Float response within an array: numerical and experimental comparison. In: Second International Conference on Ocean Energy, Brest, France.
- Vicente, P.C., Falcão, A.F.de O., et al., 2009. Dynamics of arrays of floating point-absorber wave energy converters with inter-body and bottom slack-mooring connections. *Appl. Ocean Res.* 31 (4), 267–281.
- WAMIT, 2011. WAMIT, Inc.—The state of the art in wave interaction analysis. Retrieved from [www.wamit.com](http://www.wamit.com) (accessed 28.04.11).